Elucidating the electron transport in semiconductors via Monte Carlo simulations: an inquiry-driven learning path for engineering undergraduates

IOP Publishing European Journal of Physics
Eur. J. Phys. **36** (2015) 055017 (19pp) doi:10.1088/0143-0807/36/5/055017

Elucidating the electron transport in semiconductors via Monte Carlo simulations: an inquiry-driven learning path for engineering undergraduates

Dominique Persano Adorno, Nicola Pizzolato and Claudio Fazio

Physics Education Research Group, Dipartimento di Fisica e Chimica, Università di Palermo, Italy

E-mail: dominique.persanoadorno@unipa.it

Received 16 February 2015, revised 26 April 2015
Accepted for publication 1 June 2015
Published 15 July 2015

Abstract

Within the context of higher education for science or engineering undergraduates, we present an inquiry-driven learning path aimed at developing a more meaningful conceptual understanding of the electron dynamics in semiconductors in the presence of applied electric fields. The electron transport in a nondegenerate n-type indium phosphide bulk semiconductor is modelled using a multivalley Monte Carlo approach. The main characteristics of the electron dynamics are explored under different values of the driving electric field, lattice temperature and impurity density. Simulation results are presented by following a question-driven path of exploration, starting from the validation of the model and moving up to reasoned inquiries about the observed characteristics of electron dynamics. Our inquiry-driven learning path, based on numerical simulations, represents a viable example of how to integrate a traditional lecture-based teaching approach with effective learning strategies, providing science or engineering undergraduates with practical opportunities to enhance their comprehension of the physics governing the electron dynamics in semiconductors. Finally, we present a general discussion about the advantages and disadvantages of using an inquiry-based teaching approach within a learning environment based on semiconductor simulations.

Keywords: inquiry-based learning, Monte Carlo simulations, III–V semiconductors

(Some figures may appear in colour only in the online journal)

1. Introduction

In recent years, there has been considerable interest in indium phosphide (InP) and related alloys because of their applications in many electronic and photonic devices. The progress made over recent decades in the preparation and processing of InP-related materials has allowed the development of highly reliable devices in the field of optoelectronics technology. The ternary alloy, GaInAs, and the quaternary alloy, GaInAsP, grown in lattices matched to InP substrates, are the materials of choice for making light sources and detectors for high-data-rate, long-haul, highly efficient fibre-optic communication systems [1]. High-speed hetero-junction bipolar transistors and high-electron mobility transistors are being realized from GaInAs/InP and GaInAs/AlInAs hetero-structures [2]. Because of these myriad applications, InP-related materials have increased their importance inside the class of III–V semiconductors [3]. For all these reasons, a deeper understanding of the peculiarities of the electron transport dynamics in InP semiconductors is becoming essential in undergraduate education for electronic engineering and semiconductor science.

Traditional lecture-based instruction for solid state physics and electronics provides students with a theoretical background regarding the band structure and energy gaps, the concept of effective mass and the basic mechanism of phonon-induced scattering mechanisms. However, an effective and efficient engineering instruction should be able to guide students towards full comprehension of the fundamental concepts of semiconductor science and, at the same time, develop and strengthen their reasoning skills and transversal abilities, enabling graduates to immediately engage in engineering practice and related technologies ([4] and references therein). Graduate engineers should be able to demonstrate specialist-discipline knowledge, the ability to solve practical engineering problems and design skills based on innovative thinking [5–8].

In the science education field, many reports have proposed a new vision of scientific instruction, suggesting a switch from passive lecture-style teaching to a more active and student-centred teaching strategy [9–13]. In this context, inquiry-based science education represents a natural framework for developing opportunities to learn science concepts with the active construction of meaningful knowledge and stimulation of high levels of critical thinking skills [14, 15]. In inquiry-based learning, students are engaged in identifying relevant questions, searching for information, collecting data and evidence (in both laboratory and real-life environments), building descriptions and explanatory models, and communicating and sharing findings. A pure theoretical approach is not entirely successful in teaching physics, because any mental construction, i.e. any mental model [16], is based on experience and students rarely fully understand a theory, even if it is currently accepted, if it remains distant from direct experimentation [17]. Unfortunately, the technology necessary to explore electron dynamics within a semiconductor in detail is still far from being available in didactical laboratories and for this reason inquiry-based instruction seems to be an unviable learning route for students approaching the study of semiconductor properties. Nevertheless, the study of physical systems via numerical simulations can be considered as a practice that is in-between theory and experimentation [18]. Among others, the Monte Carlo (MC) method is widely recognized as an effective computational technique in condensed matter physics and, more specifically, in semiconductor research [19–21], where it can be considered to be one of the most powerful techniques to simulate charge carrier transport in semiconductor structures and devices.

In this paper we present and discuss an inquiry-based learning path for science or engineering undergraduates studying the electron transport dynamics via MC simulations in InP semiconductor bulks. This work is new with respect to others presenting semiconductor

models based on MC simulations [22], because here the main focus is not on the model itself, which is considered to be a well-established starting point, but the sequence of reasoned explorations, carried out within a scaffolding environment aimed at stimulating an effective understanding of the physics concepts underlying the complex world of semiconductor electronics. Nevertheless, this learning path represents a powerful instrument for educators introducing young undergraduates to the efficacy of MC simulations for inquiry into a physical system where the theoretical processes are well understood, but analytical investigation methods still only provide approximate results.

This paper is organized as follows. In section 2, we briefly introduce the theory of electron transport, present the model of InP and the band structure to be taken into account, discuss the details of the simulation process and report a validation of the simulated dynamics through direct comparison with published experimental data. In section 3, the results from the inquiry-driven learning sequence of numerical experiments, carried out under three different sets of physical conditions, are shown and discussed extensively. Concluding remarks are given in section 4.

2. The model

2.1. Electrons in a crystal and the InP band structure

In this section we briefly review the basic conceptual knowledge that students should hold in order to be actively involved in this inquiry-driven, simulation-based learning path on electron transport in semiconductors. Understanding the theory of carrier dynamics in a crystal and the way such theory can be effectively translated into transport simulations may be very complicated.

Electrons in semiconductor crystals move in a periodic potential, due to the periodic arrangement of atoms in a crystal. Therefore, in the study of electron transport in a semiconductor we deal with an extremely complicated many-body problem. Nevertheless, if we assume that the effect of the atomic nuclei and the remaining electrons on a selected carrier could be approximated by a given potential $\mathrm{V}(\vec{r})$, having the same periodicity as the underlying Bravais lattice, the many-body problem can be reduced to that of a single particle [23, 24]. The electron dynamics in the crystal is determined by the Schrödinger equation:

$$\left[-\frac{\hbar^2}{2m}\nabla^2 + \mathrm{V}(\vec{r})\right]\psi(\vec{r}) = \epsilon\psi, \tag{1}$$

with the periodic potential having the form:

$$\mathrm{V}(\vec{r}) = \mathrm{V}\left(\vec{r} + \vec{R}\right) \tag{2}$$

for any vector $\vec{R}$ of the appropriate Bravais lattice. Bloch's theorem states that the eigenfunctions of the Schrödinger equation for a periodic potential can be written as

$$\psi_{\vec{k}}(\vec{r}) = \exp\left(\mathrm{i}\vec{k}\vec{r}\right)u_{\vec{k}}(\vec{r}), \tag{3}$$

with the product of a plane wave $\exp\left(\mathrm{i}\vec{k}\vec{r}\right)$ and a function $u_{\vec{k}}(\vec{r})$ with the same periodicity as the lattice itself, where $\vec{k}$ stands for the electron wave vector [23, 24].

The Schrödinger equation in the simple Kronig–Penney model, which represents the crystal periodic potential seen by the electrons as a 'piecewise constant' potential, gives rise to allowed bands of energy separated by forbidden bandgaps [24]. The E-k relation is called

the band structure of the semiconductor. The gap separating the highest filled band (the valence band) from the lowest unoccupied band (the conduction band) is the well-known bandgap of the semiconductor. The form of the electron energy band structure is usually complex and, thus, quite difficult to account for without approximation. The core of modern knowledge of the electronic and optical properties of solid-state materials is based on the band theory, which describes the properties of electrons in a periodic potential.

InP is a binary semiconductor composed of indium and phosphorus. It crystallizes in a face-centred cubic ('zinc-blende') crystal structure, identical to that of gallium arsenide (GaAs) and most of the III–V semiconductors [25, 26]. InP is used in high-power and high-frequency electronics because of its superior electron velocity with respect to the more common semiconductors, silicon and GaAs. It also has a direct bandgap, making it useful for optoelectronic devices like laser diodes [25]. Moreover, InP is of great importance for quantum nanostructures due to its ability to exhibit quantum effects with relative ease, this being largely due to its low electron effective mass [26].

The three-valley model is the most commonly used approach for modelling the conduction band in an n-type InP semiconductor. A valley can be intuitively defined as a region of the conduction band containing a relative minimum. Two or more valleys are equivalent if they are centred at symmetric points of the first Brillouin zone and thus lie at the same height with respect to the energy axis. The lowest conduction valley occurs at the Γ point and is termed the Γ valley. Above this and in increasing order of energy, there appear two sets of equivalent valleys: four L valleys, centred at L points along Λ lines and three X valleys, centred near X points along Δ lines [27].

2.2. Electron dynamics and the Boltzmann transport equation

Once the E versus k relation is well established, we can, for all practical purposes, forget about the crystal potential and treat the electrons inside a crystal just like electrons in free space, except for a change in their mass, taking into account the global effect of the crystalline field only in the renormalization of the free electron mass [24].

In a perfect crystal the electrons behave just as they do in free space and suffer no scattering. But in real materials electrons do suffer scattering from all the various scattering processes. These may involve ionized impurities, alloy disorder, lattice vibrations, etc Each possible scattering process is usually described through the respective scattering rate $W_n(k, k')$ (n being the process index) at which an electron with initial wave vector k is scattered into a final state with wave vector k'. First-order time-dependent perturbation theory can be applied successfully in order to derive $W_n(k, k')$ for each n by means of the Fermi golden rule [20, 24]. In the presence of an applied electric field the electron, between two consecutive collisions, moves under the driving field as a free particle, obeying Newton's equation of motion with free electron mass replaced by its effective mass.

The probability distribution function for particles in the 6-dimensional phase space of position and crystal momentum

$$f\left(\vec{k}, \vec{r}, t\right)\frac{\mathrm{d}^3k}{(2\pi)^3}\,\mathrm{d}^3r \tag{4}$$

follows the Boltzmann transport equation (BTE), an integral-differential kinetic equation, whose solution provides the correct theoretical description of electron transport [24]:

$$\left(\frac{\partial}{\partial t} + \vec{r} \cdot \nabla\vec{r} + \vec{\dot{k}} \cdot \nabla\vec{k}\right) f\left(\vec{k}, \vec{r}, t\right) = \left(\frac{\partial f}{\partial t}\right)_{\text{coll}}, \tag{5}$$

where the right side is the rate of change of the distribution function due to randomizing collisions:

$$\left(\frac{\partial f}{\partial t}\right)_{\text{coll}} = \int \frac{\mathrm{d}^3 k'}{(2\pi)^3} W\left(\vec{k}, \vec{k}'\right)\left[f\left(\vec{k}', \vec{r}, t\right) - f\left(\vec{k}, \vec{r}, t\right)\right], \tag{6}$$

i.e. an integral over the in-scattering and out-scattering terms in momentum wavevector space. The left side of equation (5) accounts for both a diffusive term representing the diffusion of electrons and a term corresponding to the forces exerted on the particles by an external influence (not by the particles themselves)—for a detailed derivation and description see appendix B of [24]. The BTE is a semi-classical equation in the sense that particles are treated as having distinct position and momentum in violation of the uncertainty relation, but their dynamics and scattering processes are quantum-mechanically treated through the electronic band structure and the use of time dependent perturbation theory. Once $f\left(\vec{k}, \vec{r}, t\right)$ is known, physical observables, such as the average velocity, can be calculated by averaging over the distribution function.

The Boltzmann equation is a very complicated differential equation and the search for its analytical solutions is a formidable and still unsolved mathematical problem. Even if one restricts its investigation to the linear response of the material to an external field and uses a model taking into account very simple scattering mechanisms, further approximations are required in order to obtain analytical solutions. But unfortunately these provide unrealistic results. The situation is even worse in the nonlinear regime, as in the case of hot electron problems, in which one aims to study the system response to very intense electric fields or under cyclostationary conditions. In these cases the equation can only be treated numerically. Approximate solutions can be obtained within the drift–diffusion and hydrodynamic models, but the validity of these models is very limited [28, 29].

2.3. The Monte Carlo approach and simulation details

The MC approach represents one of the most powerful methods to numerically simulate transport properties in semiconductor devices, beyond quasi-equilibrium approximations. This technique, representing a space–time continuous solution of the field and transport equations, is suitable for studying both the steady state and the dynamic characteristics of the device. The MC method uses random numbers to take into account the mechanisms of interaction in a physical system at the microscopic level, providing a concrete opportunity to obtain detailed information regarding the physical phenomenon, investigated under different conditions [19–21]. Owing to its flexibility, this approach offers the remarkable advantage of providing a detailed description of the particle motion in the semiconductor, by taking into account the main details of band structure, scattering processes and heating effects, specific device design and material parameters. It allows us to obtain important electron dynamics information, such as the average velocity, temperature, current density, etc, directly and without the need to calculate the electron distribution function first. The time interval between two collisions (time of free flight), the scattering mechanisms, the collisional angle and all the parameters of the problem are chosen in a stochastic way, effecting a mapping between the probability density of the given microscopic process and a uniform distribution of random numbers [19–21].

In general, if $p(\phi)$ e $p(r)$ are the probability density functions associated with ϕ in the complex physical distribution and r in the pseudo-random distribution, respectively, it holds the identity

$$\int_0^{\phi} p(\phi')\mathrm{d}\phi' = \int_0^{r} p(r')\mathrm{d}r', \tag{7}$$

since for the uniform distribution $p(r) = 1$, we obtain

$$r = \int_0^{\phi} p(\phi')\mathrm{d}\phi'. \tag{8}$$

If the integral of $p(\phi)$ can be computed easily analytically, the inversion of equation (8) (by expressing ϕ as a function of r) gives random values for the physical variable ϕ in terms of random numbers, uniformly distributed between 0 and 1. A single-particle MC method allows us to simulate the ensemble of electrons by monitoring the history of a single carrier undergoing many scattering events in the momentum space. Therefore, it can be used to calculate the transport properties of electrons in homogeneous bulk semiconductors under static and uniform electric fields. In this case, the relevant physical quantities are computed as the time average over long temporal sequences, since as the simulation time goes on, the results become more precise. On the other hand, an ensemble MC method, based on the successive and simultaneous simulation of the dynamics of many particles during a small time interval, allows the analysis of carrier diffusion, carrier transport in inhomogeneous fields, non-stationary behaviour of electrons and so on. In this latter case, the mean quantities of interest are estimated as ensemble averages, and the temporal evolution of them can also be investigated. In order to allow our students to explore and discuss the transient phase of electron motion, we adopted an ensemble MC approach in our learning path.

In particular, our MC simulations are carried out by performing the following sequential steps.

(1) First of all, the initial condition of the system is set. Starting from a Maxwellian distribution, depending on the lattice temperature, a kinetic energy and a momentum with random direction are given to each electron.
(2) Then, the free flight time of each electron is chosen with a probability distribution determined by the scattering probabilities. The total scattering rate $W[k(t)]$ is given by

$$\mathrm{W(k)} = \sum_{\mathrm{i}=1}^{\mathrm{m}} \lambda_{\mathrm{i}}(\mathrm{k}), \tag{9}$$

where m is the total number of scattering mechanism and $\lambda_{\mathrm{i}}(\mathrm{k})$ is the individual scattering rate. The probability per unit time that the electron will drift before a scattering event is given by [19–21]:

$$\mathrm{P(t)} = \mathrm{W[k(t)]}\ \exp\left\{ -\int_0^{\mathrm{t_f}} \mathrm{W[k(t)]\,dt} \right\}. \tag{10}$$

By using the mapping between the probability density of this microscopic process and a uniform distribution of random numbers (see equation (8)), we obtain the equation

$$\mathrm{r} = 1 - \exp\left\{ -\int_0^{\mathrm{t_f}} \mathrm{W[k(t)]\,dt} \right\}, \tag{11}$$

where r is a random number uniformly distributed between 0 and 1. If the integral in equation (11) cannot be trivially evaluated, a good expedient is to utilize the self-scattering method [20]. In this procedure, a fictitious scattering mechanism, whose rate always adjusts

itself in such a way that the total (self-scattering plus real scattering) rate is constant in time to a fixed value Γ, is introduced. The self-scattering mechanism, when selected as the free flight terminating mechanism, does not change the electron state and has no effect on the particle trajectory, but it allows the simplification of equation (10) in the form

$$P(t) = \Gamma e^{-\Gamma t}. \tag{12}$$

The constant Γ is chosen so that it is larger than the maximum scattering rate encountered during the simulation interval. With this simplification the variable r is given by

$$r = 1 - e^{-\Gamma t} \tag{13}$$

and the free flight time can be computed easily.

During the free flight the applied force changes the momentum of the electron according to the relation

$$k(t) = k(0) - \frac{eEt}{\hbar}, \tag{14}$$

where E is the electric field vector component directed in the **x**, **y** or **z** direction.

(3) A scattering event is randomly selected for each electron.
(4) The new energy value (in case of inelastic scattering) and scattering angles of electron momentum are calculated.
(5) The simulation continues from point 2 until the final condition is achieved.

At fixed sampling time steps, small enough to properly update the particle motion, ensemble average values of the physical quantities of interest, such as electron velocity and temperature, are calculated.

In this work the electron dynamics is studied in a crystal of infinite dimensions (bulk or 3D), in which the charge carriers are subject to the action of a static electric field. We adopted the three-valley model with an isotropic band structure and, therefore, in each valley only a value for the effective mass is employed. Our model takes into account the non-parabolicity of the InP band structure and the intervalley and intravalley scattering of electrons in multiple energy valleys. In particular, it includes: (i) the intravalley scattering with acoustic phonons, ionized impurities, acoustic piezoelectric phonons, polar optical phonons, and for the L valleys also the scattering with optical nonpolar phonons; (ii) the intervalley scattering with optical non-polar phonons among the three valleys [30, 31]. The scattering probabilities are calculated using the Fermi golden rule and are assumed to be field independent. Accordingly, the influence of the external field is only indirect through the field-modified electron velocities [30, 31]. Examples of MC codes taking all these scattering mechanisms into account can be found in [20, 32].

In figures 1(a) to (e) we show how the electron scattering rates change with the electron energy in the different valleys at lattice temperature $T = 300\,K$ and impurity density $n = 10^{13}\,m^{-3}$. In particular, the scattering rates due to the acoustic phonons (figure 1(a)), ionized impurities (figure 1(b)), emission of polar and non-polar optical phonons (figure 1(c)), absorption of polar and non-polar optical phonons (figure 1(d)) and the total scattering rate (figure 1(e)), are shown. Students should be invited to note and discuss the presence of a threshold energy for the phonon emission process in the Γ valley. Moreover, it is important to highlight that for high energy electrons the scattering rates due to both absorption and emission of optical phonons are not strongly dependent on the electron energy and that the probability of scattering with the emission of optical phonons is several times larger than it is for the absorption process [20].

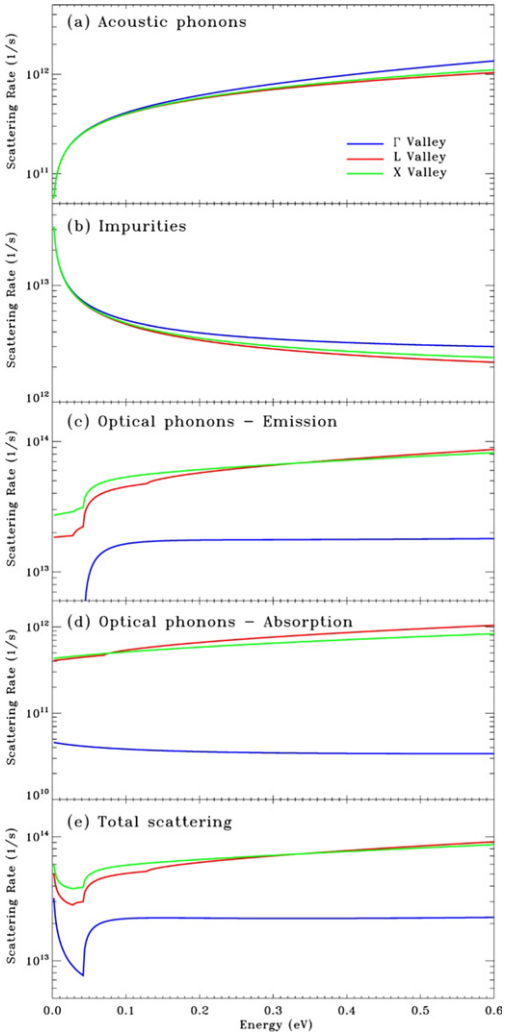

Figure 1. Scattering rates as a function of the energy for electrons moving within an InP semiconductor bulk at lattice temperature T = 300 K and impurity density $n = 10^{13}$ m^{-3}. (a) Acoustic phonons, (b) ionized impurities, (c) emission of polar and non-polar optical phonons, (d) absorption of polar and non-polar optical phonons and (e) the total scattering rate for electrons in the Γ (blue lines), L (red lines) and X (green lines) valleys.

In our numerical experiments, we consider electrons as independent particles, neglecting electron–electron interactions, which are not influential for transport properties. All simulation results are recorded after a transient time of a few picoseconds has elapsed and a stationary regime has been achieved. In our range of lattice temperatures ($80 < T < 300$ K) and for the values of impurity density investigated here, the Fermi temperature is much smaller than the electron temperature and, therefore, degeneracy does not play a relevant role. We assume that all donors are ionized and that the free electron concentration is equal to the doping concentration. The complete set of parameters used in this work is given in table 1.

Table 1. Set of *n*-type InP semiconductor parameters used in our calculations [33, 34].

Density, kg m^{-3}			4790
Sound velocity, m s^{-1}			5130
Dielectric constant (high frequency)			9.56
Dielectric constant (low frequency)			12.40
Piezoelectric constant, C m^{-2}			0.035
	Γ valley	L valley	X valley
Effective mass	0.078	0.260	0.325
Not parabolicity coefficient eV^{-1}	0.83	0.23	0.38
Energy gap	0	0.86	0.96
Number of equivalent valleys	1	4	3
Acoustic deformation potential, eV	6.5	6.5	6.5
Optical deformation potential, 10^{10} eV m^{-1}	—	6.7	—
Intervalley deformation potential, 10^{10} eV m^{-1}			
Γ valley	—	10	10
L valley	10	10	9
X valley	10	9	9
Polar optical phonon energy, eV	0.0422	0.0422	0.0422
Optical not polar phonon energy, eV	—	0.0432	—
Intervalley phonon energy, eV			
Γ valley	—	0.0278	0.0299
L valley	0.0278	0.0290	0.0293
X valley	0.0299	0.0293	0.0299

2.4. Model validation

In the context of any simulative study, the first step to be carried out by researchers regards the validation of the model. Even considering the case where students are not asked to participate in the model development phase, they should understand that, before starting to use a model developed by others, they should always check its validity. In this respect, the educators should stimulate the students to question themselves about the necessity for a model validation process, by letting them reflect on the importance for a given model to reproduce the realistic behaviours of a physical system, by focusing on the necessity and opportunity for scientists to model real-world phenomena. They would understand that the validation of a model requires a comparison between its computational outcomes and the data gathered by others via experimental measurements. In this phase, the students have to carefully check the conditions under which the experiments reported in the literature were carried out, such as the lattice temperature and carrier density in this specific context, in order to set the correct parameters in their model before running their simulations. They also have to understand that any experimental result is affected by uncertainties and, for this reason, they will not ever find a perfect agreement among the several data coming from different experiments.

Here, the validation process was performed by investigating how the average electron drift velocity at lattice temperature $T = 300$ K changes as a function of the driving electric field. In particular, in figure 2 the experimental data collected by Glover *et al* (triangles), Nielsen (diamonds) and Hayes (asterisks) [35–37] are compared with our numerical findings (green squared), obtained by averaging the ensemble means of the electron drift velocity over the total temporal length of the simulation, with the exclusion of a transient time of 50 ps. This interval, empirically estimated by observing the time evolution of the electron drift

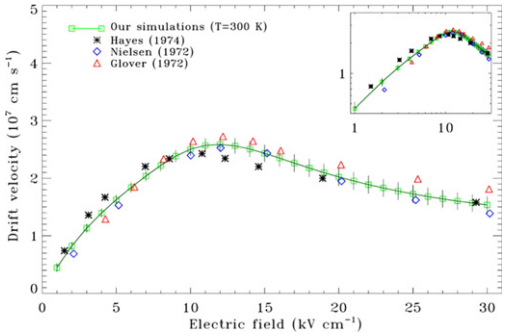

Figure 2. Comparison between our simulations (green squared) and experimental data collected from by Glover *et al* (triangles), Nielsen (1972) (diamonds) and Hayes (1974) (asterisks) [35–37]. The vertical lines overlying on the green squared symbols provide the statistical errors associated with the computed average values of the drift velocity. The inset shows the comparison between the experimental and simulated data on a log–log scale.

velocity, has been removed from the initial phase of the simulation because the mean drift velocities exhibit large transient overshoots before the steady state values are reached [20]. In figure 2, the error bars overlying the green squared symbols represent the standard deviation of the ensemble means of the electron drift velocity. Both the number of particles (10^4) and the total duration of the simulations (1 ns) have been chosen to guarantee statistical errors comparable to the dispersion observed in the experimental data.

In this phase, the students should concentrate their attention on the capacity of their simulated data to reproduce the corresponding experimental values closely, leaving the effective understanding of the physics beyond their findings to a subsequent explanatory phase. The agreement between the numerical and experimental data shown in figure 2 can be considered to be satisfactory over the whole range of investigated values of electric field, providing the required validation of the MC model. More generally, however, the students might be interested to further improve their model in order to minimize the observed discrepancies between its numerical outcomes and the experimental findings. In this case, the educators should drive the students' inquiry towards the exploration of those model parameters that can be opportunely tuned to achieve this goal.

The model used in this work, whose results are shown in figure 2, was developed by following this calibration process correctly, which led to the set of parameters listed in table 1.

3. Results

In this section we report the results of a series of simulations that a class of science/engineering undergraduates might be interested in performing, with the aim of elucidating the role of important physical quantities—such as the crystal temperature, effective mass and doping concentration—on the electron transport dynamics. In the following, an inquiry-based approach is suggested for scaffolding student investigations throughout the several scenarios they may encounter during their learning paths. The general problem driving students' questioning deals with the exploration of the concrete chances of improving the electron transport dynamics, in terms of an increase of the signal speed, i.e. carrier velocity, with respect to the lower achievable maintenance cost, i.e. the driving electric power. The

teaching/learning path is outlined in the next three subsections. Each one starts from a reasoned question and describes a set of simulative experiments whose results are explicative at some level of understanding and, at the same time, boost the learners' thinking with further questions to be addressed by a deeper scientific inquiry.

3.1. Which physical quantities affect the velocity-field characteristics?

The first question driving student inquiry into the electron dynamics within a semiconductor regards the observed features of the electron velocity-field characteristics. We performed our calculations by simulating the electron transport within an InP bulk characterized by an impurity concentration (free electron concentration) $n = 10^{13}\,\mathrm{m}^{-3}$ (low-doped regime) and a driving electric field ranging between 1 and 30 $\mathrm{kV\,cm}^{-1}$.

In figure 3(a) we show how the electron drift velocity, averaged over an ensemble of 10^4 charge carriers, changes as a function of the driving electric field. These data have been obtained at two different lattice temperatures, T = 77 K (triangles) and 300 K (squares), respectively. However, before being engaged in the comprehension of the temperature effect on electron dynamics, the students' questioning should be driven towards a deeper understanding of the general features shown by the electron drift velocity as a function of the field amplitude.

The overall analysis of both curves shown in figure 3(a) highlights the presence of nonlinear velocity-field characteristics, where an initially increasing phase of the electron drift velocity is followed by a maximum at about 10 $\mathrm{kV\,cm}^{-1}$ and a subsequent negative differential region, characterized by a decreasing drift velocity for higher values of the electric field. This first result could represent a surprise for students, who probably expect to see the well-known ohmic behaviour. In effect, in the low field region the velocity-field dependence resembles the familiar Ohm's law, while significant deviations from it are clearly evident at stronger electric fields. The educators should stimulate the students to inquire about this phenomenon, in order to address the physical reasons behind the observed decrease of the electron drift velocity.

By considering that the electron energy is expected to be related to the electron velocity, the students might be interested to see how the average electron energy changes at different values of the driving electric field (figure 3(b)). For electric fields in the range 1–8 $\mathrm{kV\,cm}^{-1}$, the energy increases slowly up to about 0.1 eV. Higher driving fields cause a rapid enhancement of the electron energy up to a saturation regime at about 0.4 eV. This result may be doubly surprising for students, who firstly expect that the kinetic energy should always follow the electron velocity characteristics, consequently dropping as the mean velocity does, and secondly do not expect a saturation of the energy levels, but eventually an increase for higher driving fields.

At this stage, a further discussion should be stimulated by the instructors regarding how this phenomenon can be physically explained and, in particular, the students should question whether the energy–field relation found provides a useful complementary view of the electron dynamics, by adding some more scientifically relevant details with respect to the velocity-field characteristics. The comparison between (a) and (b) of figure 3 does not provide a direct view of the causal relation between the electron energy and the electron drift velocity, in particular in the region of electric field amplitudes greater than 10 $\mathrm{kV\,cm}^{-1}$. Therefore, a deeper inquiry is needed: 'what really happens to the electron ensemble at higher electric fields?'

At least at the theoretical level, the students should know that electrons moving within a semiconductor may occupy different valleys, depending on their energy, and they should

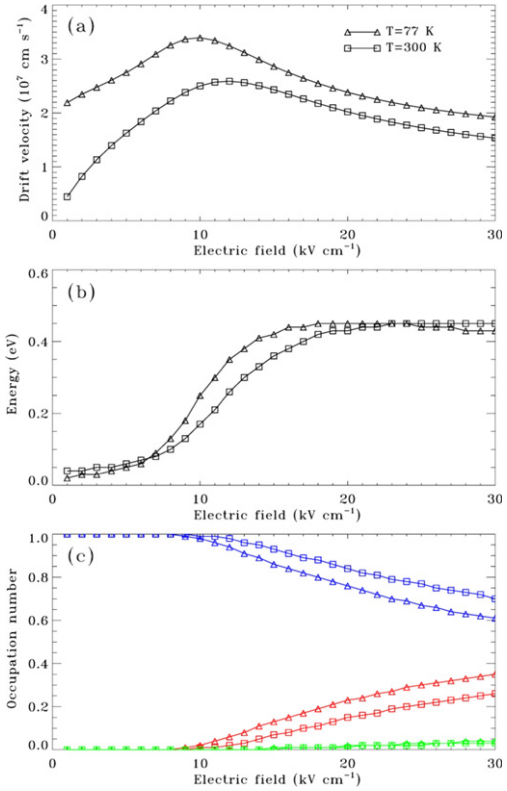

Figure 3. Averages of drift velocity (a), kinetic energy (b) and occupation number (c) as a function of the driving electric field for MC simulations of electron transport in InP with impurity density $n = 10^{13}$ cm^{-3}, at temperatures T = 77 K (triangles) and 300 K (squares). In (c) blue, red and green are used to represent the occupation in the Γ, L and X valleys, respectively.

have already studied that electrons in different valleys are characterized by different effective masses. In the absence of an applied electric field, the electrons are in equilibrium with the crystal lattice, which has a mean energy of the order of k_BT J, where T is the lattice temperature and k_B is the Bolzmann's constant $1.38{\cdot}10^{23}$ J/K^{-1}. Therefore, $E_{latt}(T = 77\ K) \sim 0.01$ eV, $E_{latt}(T = 300\ K) \sim 0.03$ eV. The application of an electric field causes the electrons to cease to be in equilibrium with the crystal lattice and it increases their energy until it is possible for them to transfer from the Γ valley to the higher energy L and X valleys, where the effective mass is greater (heavy electrons). The electron transfer from the Γ valley to the upper valleys may be confirmed by the observation of the electron occupancy in each valley. The activation of this cognitive resource may provide the students with the useful suggestion to explore how the occupation numbers of the electron ensemble change as a function of the electric field (figure 3(c)). As expected, the electron population in the Γ valley decreases with the increase of the applied field, while that in the L and X valleys increases. At this stage, the students may note that electrons start to populate the higher valleys when the electric field amplitude reaches values greater than about 10 kV cm^{-1}, with the same value characterizing the maximum of the velocity-field characteristics. Even without providing a direct explanation of the observed velocity- and energy-field characteristics, this finding

supports the importance of taking into account the effective mass of charge carriers and the fundamental role played by scattering events, which are ultimately responsible for intervalley transitions. Here, the characteristic cycle of inquiry-based learning, starting from student engagement and caused by an unexpected result, then evolving through a series of investigations based on simulated experiences that support the working hypothesis, now closes with an explicatory phase where the students are stimulated to share their views and discuss the convincing evidence with each other. In particular, concerning the energy saturation, the students should be able to link this finding to the fact that the electrons initially remain in the Γ valley, where they gain much energy because of the low effective mass of that valley. When they gain enough energy to transit to the L and X valleys, the mean kinetic energy saturates, since part of the energy of the carriers present in the Γ valley is converted into potential energy on passing to the upper ones. This line of reasoning should drive the students towards a search for literature data at higher fields in order to find out where the electric field compensates the effects of the intervalley mechanisms (above $50\,\mathrm{kV\,cm^{-1}}$), allowing the electron mean kinetic energy to grow again steadily with the field.

Our MC simulations have also highlighted that the average electron drift velocity obtained at room temperature is lower than the corresponding quantity at $\mathrm{T} = 77\,\mathrm{K}$ in the whole range of investigated values for the electric field (figure 3(a)). Even the average energy of electrons at $\mathrm{T} = 300\,\mathrm{K}$ is lower than the electron energy at $\mathrm{T} = 77\,\mathrm{K}$, at least in the range of electric field amplitudes of about $[6 \div 23]\,\mathrm{kV\,cm^{-1}}$, while slightly higher values are found at lower and higher electric fields (figure 3(b)). The students' inquiry should be driven by the educators towards a critical analysis of this effect. As a matter of fact, carrier motion in semiconductor crystals is made up of a succession of scattering events and drift processes. Therefore, the dependence of the electron velocity-field characteristics on the temperature is expected to be related to the different strength of the interactions between charge carriers and lattice vibrations, i.e. phonons. The students should note that the phonon scattering probability increases with the enhancement of the crystal temperature, contributing to a faster energy and momentum relaxation process. Since the number of phonons in a crystal increases with the lattice temperature, students should expect that the mobility decreases at higher temperatures.

The analysis of the outcomes from these first numerical experiments may provide the students with a clearer view of the semiconductor's response to an external driving field, confirming the theoretical background regarding phonon interactions, without specifically entering into the detailed quantum calculation of the scattering probabilities, usually carried out using Fermi's golden rule.

3.2. A deeper inquiry: how do intervalley transitions affect the results and what role does the effective mass play?

The MC simulation outcomes shown in the previous subsection highlighted a clear connection between the observed velocity-field characteristics and the electron ensemble occupation number, unveiling the fundamental role played by intervalley transitions in electron transport dynamics. This section is aimed at providing a deeper exploration of these phenomena by fully exploiting the potential of the MC numerical method, which is a powerful instrument with which to investigate electron transport in semiconductors, even under those unrealistic physical conditions that cannot be explored during a real laboratory experiment, but whose accomplishment could help students to better understand the underlying physics. Within this framework, an inquiry-based approach is followed to provide both educators and learners with the necessary teaching/learning scaffolding structure to deeper investigate the

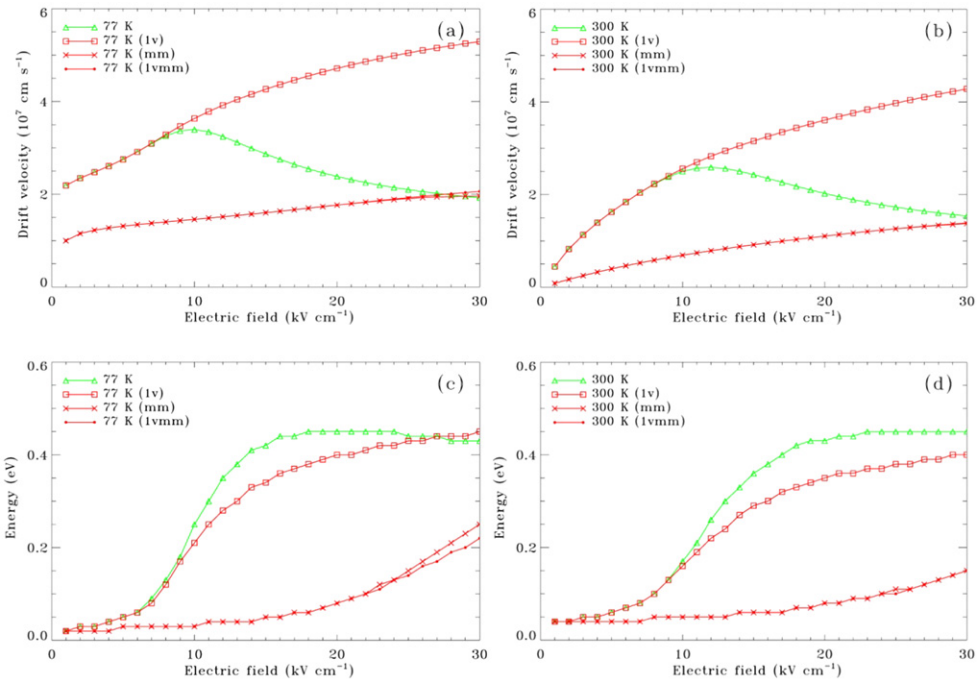

Figure 4. Averages of drift velocity (a), (b) and kinetic energy (c), (d) as a function of the applied electric field, for MC simulations of electron transport in InP with impurity density $n = 10^{13}$ cm^{-3} at temperatures $T = 77$ K (left) and 300 K (right). Results obtained from four different modellings of the band structure are compared: (i) three-valley model (green triangles); (ii) single-valley model (red squares, labelled '1v'); (iii) three-valley mean-mass model (asterisks, labelled 'mm'), where the electron mass in all valleys is set as equal to the mean value among the three effective masses listed in table 1; and (iv) single-valley mean-mass model (dots, labelled '1vmm'), with the same effective mass as above.

effects of intervalley transitions and effective mass on electron transport dynamics. Students may ask 'how can we be sure that the observed maximum in the velocity-field characteristics can be ascribed to intervalley transitions?' Here, this question is addressed by performing MC simulations for electrons driven within an InP bulk semiconductor at temperatures of 77 and 300 K by a static electric field, ranging between 1 and 30 kV cm^{-1}, but this time forcing all electrons to remain in the Γ valley, independently of their energy.

In figure 4 we show a comparison between the results obtained using the three-valley model as shown in the previous subsection (green triangles) and those coming from the single-valley (Γ) model (red squares, labelled '1v'), in which the electron transitions to higher energy valleys are inhibited.

The single-valley data of the electron drift velocity (red squares in figures 4(a) and (b)) describe an increasing trend in the whole range of investigated values for electric field, without showing the maximum observed in the results coming from running a multivalley model. By forcing all electrons to remain within the lower energy band, students may have the opportunity to assert that the decrease of the electron drift velocity observed at fields greater than 10 kV cm^{-1} can be definitely ascribed to the electron transitions up to higher energy valleys. In fact, for field amplitudes lower than the threshold field (Gunn field), where

all the electrons are in the Γ valley, the two plots coincide. The transfer to higher valleys becomes possible if the electrons acquire an energy greater than the width of the gap. In the single-valley case, for values of the electric field greater than the Gunn field, the drift velocity of electrons increases monotonically. As expected, this result is mirrored by the mean electron energy, which does not reach the saturation plateau previously observed, but shows a slight increasing trend (red squares in figures 4(c) and (d)).

A reasoned inquiry about the physics behind this phenomenon will guide learners through a deeper exploration of the role played by the effective mass of drifting electrons and, in particular, the inertial response of the system due to the change of the effective mass in higher valley electrons. Here, we report the results from a numerical experiment that students may be interested in carrying out in order to investigate the effects of considering that all electrons have the same mass, but this time equal to the average value among the effective masses listed in table 1 for different valleys. In figure 4, asterisks and dots are used, respectively, to show the results from a three-valley mean-mass model (labelled 'mm'), where the ensemble electrons are still able to make intervalley transitions, and a single-valley mean-mass model (labelled '1vmm'), where intervalley transitions are inhibited. The velocity-field characteristics at both 77 and 300 K (figures 4(a) and (b)) show a similar trend, increasing linearly. As a consequence, the energy–field relationship (figures 4(c) and (d)) follows a well-defined parabolic path. Here, students cannot appreciate divergences between the multivalley and the single-valley model. As a matter of fact, the two models, labelled 'mm' and '1vmm', respectively, do not show significant differences, except for electric fields greater than 25 kV cm^{-1} at 77 K. In this regard, students should be stimulated to discuss this phenomenon —which could be attributed to the differences on the scattering rates among different valleys —among their peers and to take their inquiry further.

3.3. What effects come from a change to the impurity density?

The characteristic trend observed in the mean electron energy, which increases with the enhancement of the electric field until it reaches a plateau at about 0.4 eV, maintaining this nearly constant value up to 30 kV cm^{-1} electric field, can be explained by the fact that the energy relaxation rate due to the phonon scattering in the upper valleys is much larger than that due to the phonon scattering in the Γ valley. In this regard, the efficacy of the scattering mechanisms causing intra-valley transitions, as a function of the driving electric field, becomes the principal target for further student investigation.

In order to highlight the effect of the interactions between the free electrons and the ionized impurities, randomly distributed inside the crystal, the students can be stimulated to investigate the peculiar characteristics of the electron transport in InP at different values of doping density.

In figure 5 we show the values of the mean electron drift velocity ((a) and (b)) and the mean electron energy ((c) and (d)), obtained at two doping density values, $n = 10^{13}$ m^{-3} (green triangles) and $n = 10^{17}$ m^{-3} (red squares), at two different lattice temperatures, namely T = 77 K (left) and 300 K (right), in the presence of a driving electric field ranging between 1 and 30 kV cm^{-1}.

At both the investigated temperatures, the effect of increasing impurity scattering is relevant only in the low-field region, where a decrease of the mean drift velocity occurs. The increase of the doping density causes an increase of the momentum relaxation rate, and this is because the carrier motion is disturbed more by the scattering events in the heavier doped case. Since ionized impurity scattering appears to be very relevant for carriers mainly at low fields and/or at low temperatures, students should conclude that the impurity scattering rate

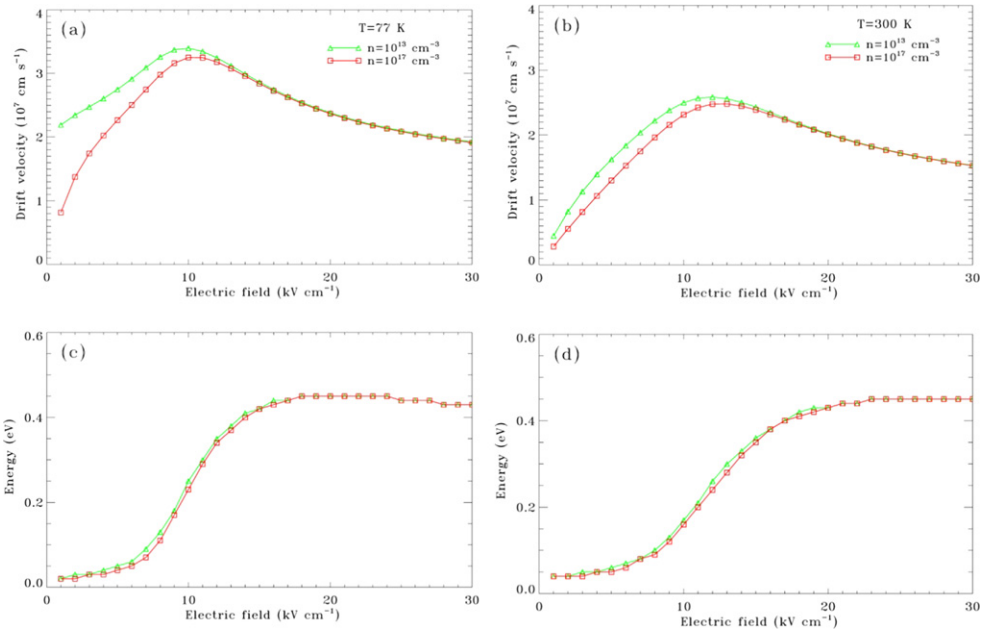

Figure 5. Averages of drift velocity ((a) and (b)) and kinetic energy ((c) and (d)) as a function of the driving electric field, for MC simulations of electron transport in InP with impurity densities of $n = 10^{13}\,cm^{-3}$ (green triangles) and $n = 10^{17}\,cm^{-3}$ (red squared) at temperatures T = 77 K (left) and 300 K (right). Here the multivalley model (taking into account the three effective masses as in table 1) is used.

decreases when the electron energy increases, becoming negligible in the high-field region. Furthermore, because the screened Coulomb potential is time independent, the electron energy must be conserved during the scattering. This implies that the mean electron energy is not affected by the impurity density level, as students can see in the lower panels of figure 5.

4. Discussion and conclusions

Knowledge of semiconductor transport properties is a fundamental instrument for any physicist or engineer involved in technology design for developing future semiconductor-based devices. However, it is widely recognized that an effective understanding of the physics governing natural phenomena cannot be achieved solely through lecture-based instruction, as adopted in many university courses on condensed matter physics; it needs to be acquired within an active framework of experimental processes. Sometimes fundamental experiments are also presented to the students, but often as a mere demonstration of already introduced concepts. The literature in the field of physics education research agrees on the benefits (and necessity) of engaging learners through inquiry-based learning paths, in order to surmount epistemological difficulties [17], achieve a more effective conceptual knowledge [5] and, at the same time, enhance students' reasoning skills [6]. Under these terms, the physics of semiconductor science could be understood at a deep level by active learners engaged in inquiry-driven experiments. Unfortunately, the setup of real experiments on semiconductors is not easily available in most university laboratories for many students. In this regard,

numerical simulation represents a valid alternative [18], but it still lacks the necessary inquiry-embedded scaffolding structure.

This paper contributes to the filling of this gap by presenting an inquiry-driven teaching/learning path for the physics underlying the transport characteristics of III–V semiconductors, by means of multi-particle MC simulation, modelling the electron transport within an InP bulk semiconductor. The MC method uses random numbers to take into account the mechanisms of interaction in a physical system at the microscopic level, providing students with a concrete opportunity to obtain detailed information regarding the physical phenomenon, investigated under several different conditions. Due to its flexibility, this approach takes into account many scattering mechanisms, specific device design, material properties and boundary conditions, allowing analysis of the characteristics of carrier dynamics under differing specific conditions.

The learning path is presented in this paper by following a scientific questioning sequence that hypothetical students engaged in an active experimental investigation of InP semiconductor transport properties could be stimulated to address. After the fundamental phase of model validation, the presentation of the simulation results is guided through a reasoned inquiry following the student point of view, aimed at strengthening their knowledge of the physical effects coming from a change in the effective mass, the band structure, crystal vibrations and impurities. Moreover, inquiry-driven MC simulation of charge carrier transport offers a very interesting teaching method for both condensed matter physics and statistical mechanics, where different physical aspects can be explored in depth.

In summary, the activation of new cognitive resources by means of inquiry-based teaching strategies, which are mainly deployed by first engaging and motivating the students and then supporting them in a process of reasoned exploration, promoting the sharing of obtained results and peer-to-peer discussions, alongside the advantages of using MC simulations to solve complex problems in a straightforward way and explore different configurations of our system model, makes this learning path a potential aid for teaching semiconductor physics more effectively.

Finally, the benefits of integrating a lecture-based method of instruction of semiconductor science with MC simulations embedded with scientific inquiry pedagogies would result in an enhancement of the ability of students to diagnose problems, critique experiments, construct models and plan alternative investigations, high-order reasoning skills that are required for future scientists and engineers.

Acknowledgments

This work was partially supported by MIUR and CNISM.

References

[1] Sloanes T J 2009 Measurement and application of optical nonlinearities in indium phosphide, cadmium mercury telluride and photonic crystal fibres *PhD Thesis* University of St Andrews (http://hdl.handle.net/10023/723)

[2] Adachi S 1992 *Physical Properties of III-V Semiconductor Compounds: InP, InAs, GaAs, GaP, InGaAs and InGaAsP* (New York: Wiley)

[3] Hayes T R 1992 *InP and Related Materials: Processing, Technology and Devices* ed A Katz (Boston: Artech House) ch 8

[4] Borrego M and Bernhard J 2011 The emergence of engineering education research as an international connected field of inquiry *J. Eng. Educ.* **100** 14

[5] Streveler R A, Litzinger T A, Miller R L and Steif P S 2008 Learning conceptual knowledge in the engineering science: overview and future research directions *J. Eng. Educ.* **97** 279
[6] Redish E F and Smith K A 2008 Looking beyond content: skill development for engineers *J. Eng. Educ.* **97** 295
[7] Nguyen D Q 1998 The essential skills and attributes of an engineer: a comparative study of academics, industry personnel and engineering students *Glob. J. Eng. Educ.* **2** 65
[8] NAE 2004 *The Engineer of 2020: Visions of Engineering in the New Century* (Washington, DC: National Academies)
[9] NRC 1996 *National Science Education Standards. National Committee for Science Education Standards and Assessment* (Washington, DC: National Academies)
[10] NRC 2000 *Inquiry and the National Science Education Standards: A Guide for Teaching and Learning* (Washington, DC: National Academies)
[11] Rocard M, Csermely P, Jorde D, Lenzen D, Walberg-Henriksson H and Hemmo V 2007 Science Education Now: A Renewed Pedagogy for the Future of Europe *EU Research Report ISSN*
[12] NAE 2010 *Grand Challenges for Engineering* (Washington, DC: National Academies)
[13] NAE 2012 *Frontiers of Engineering 2011* (Washington, DC: National Academies)
[14] Llewellyn D 2002 *Inquiry Within: Implementing Inquiry-based Science Standards* (Thousand Oaks, CA: Corwin)
[15] Wei Y, Zhai Z, Gunnarsson K and Svedlindh P 2014 A guided enquiry approach to introduce basic concepts concerning magnetic hysteresis to minimize student misconceptions *Eur. J. Phys.* **35** 065015
[16] Greca I M and Moreira M A 2000 Mental models, conceptual models and modelling *Int. J. Sci. Educ.* **22** 1
[17] Pizzolato N, Fazio C, Sperandeo Mineo R M and Persano Adorno D 2014 Open-inquiry driven overcoming of epistemological difficulties in engineering undergraduates: a case study in the context of thermal science *Phys. Rev. ST Phys. Educ. Res.* **10** 010107
[18] Li Y, Ma L and Shi Y 2011 Exploration on computer simulation method in physics education *Education and Educational Technology* vol 108 (Berlin: Springer) 517
[19] Jacoboni C and Lugli P 1989 *The Monte Carlo Method for Semiconductor Device Simulation* (Berlin: Springer)
[20] Tomizawa K 1993 *Numerical Simulations of Submicron Semiconductor Devices* (London: Artech House)
[21] Moglestue C 1993 *Monte Carlo Simulation of Semiconductor Devices* (London: Chapman and Hall)
[22] Capizzo M C, Sperandeo-Mineo R M and Zarcone M 2008 Electric conduction in semiconductors: a pedagogical model based on the Monte Carlo method *Eur. J. Phys.* **29** 451
[23] Kittel C 2004 *Introduction to Solid State Physics* 8th edn (Hoboken: Wiley)
[24] Singh J 2004 *Modern Physics for Engineers* (Weinheim: Wiley)
[25] Hilsum C and Rose-Innes A C 1961 *Semiconducting III–V Compounds* (Oxford: Pergamon)
[26] Levinstein M, Rumyantsev S and Shur M 1999 *Handbook Series on Semiconductor Parameters* (London: World Scientific)
[27] Brennan K and Hess K 1984 High field transport in GaAs, InP and InAs *Solid-State Electron.* **27** 347
[28] Vasileska D, Mamaluy D, Khan H R, Raleva K and Goodnick S M 2008 Semiconductor device modeling *Journal of Computational and Theoretical Nanoscience* **5** 999
[29] Vasileska D, Goodnick S M and Klimeck G 2010 *Computational Electronics: Semiclassical and Quantum Transport Modeling* (Boca Raton, FL: CRC Press)
[30] Persano Adorno D, Zarcone M and Ferrante G 2000 Far-infrared harmonic generation in semiconductors:a monte carlo simulation *Laser Phys.* **10** 310
[31] Persano A D 2010 Polarization of the radiation emitted in gaas semiconductors driven by far infrared fields *Laser Phys.* **20** 1061
[32] Boardman A D 1980 *Computer Simulation of Hot Electron Behaviour in Semiconductors Using Monte Carlo Methods* (Hoboken: Wiley)
[33] Persano Adorno D, Zarcone M and Ferrante G 2001 Monte Carlo simulation of harmonic generation in InP *Laser Part. Beams* **19** 81
[34] Persano Adorno D, Zarcone M and Ferrante G 2001 High order harmonic generation efficiency in *n*-type silicon and InP *Laser Phys.* **11** 291

[35] Glover G H 1972 Microwave measurement of the velocity-field characteristics of *n*-type InP *Appl. Phys. Lett.* **20** 224
[36] Nielsen L D 1972 Microwave measurements of electron drift velocity in indium phosphide for electric fields up to 50 kV cm^{-1} *Phys. Lett.* **38** 221
[37] Hayes R E 1974 Measurement of the velocity-field characteristic of indium phosphide by the microwave absorption technique *IEEE Trans. Electron Devices* **21** 233